Al-induced reduction of the oxygen diffusion in HfO$_2$: an *ab initio* study

Z F Hou[1], X G Gong[1] and Quan Li[2]

[1] Surface Physics Laboratory and Department of Physics, Fudan University, Shanghai 200433, People's Republic of China
[2] Department of Physics, The Chinese University of Hong Kong, Shatin, New Territory, Hong Kong

Abstract

Using first-principles calculations we have studied the effect of Al addition on the diffusion of interstitial oxygen atoms and ions in HfO$_2$. Calculated results show that interstitial oxygen ions in the singly negatively charged state easily diffuse in HfO$_2$ via exchange with lattice oxygen atoms, due to the lower diffusion barrier as compared to those for neutral interstitial oxygen atoms and interstitial oxygen ions in the doubly negatively charged state. The addition of Al raises the diffusion barrier for interstitial oxygen because the interstitial oxygen is strongly attracted by its neighboring Al atoms. The electronic structure analysis further reveals that the bonding between interstitial oxygen and lattice oxygen atoms is strengthened for each charge state of interstitial oxygen in HfO$_2$ with the addition of Al.

1. Introduction

The downscaling of complementary metal–oxide–semiconductor (CMOS) transistors has led to a need for alternative insulator oxides with high dielectric constant (κ) to replace SiO$_2$ as the gate dielectric, in order to maintain low gate leakage current [1, 2]. Recently, studies have demonstrated that HfO$_2$ is one of the best high-κ oxide candidates for replacement of the SiO$_2$ gate dielectric, due to its appropriate value of the dielectric constant (20–25) [2], high electron barriers [3], and good thermal stability against both silicide and silicate formation [4]. In 2006, Intel announced that hafnium based oxides had been successfully employed as gate dielectrics in conjunction with metal gates in 45 nm transistor technology [5]. However, several properties, critical for excellent performance of HfO$_2$ as a high-κ gate dielectric, depend sensitively on the behavior of oxygen [6]. In particular, The diffusion of oxygen during post-deposition thermal processing of HfO$_2$ films on silicon may lead to the growth of an uncontrollable interfacial oxide layer between the gate dielectric and silicon substrate [2, 6, 7], altering the chemical composition of the dielectric films, and consequently affect the electrical characteristics of gate stacking [8, 9]. Therefore, it is of great importance to understand the behavior of oxygen diffusion in HfO$_2$, in order to properly control the film properties under post-deposition annealing [6].

On the other hand, it is more important to look for a solution for reducing the undesirable oxygen diffusion in HfO$_2$. Considering that Al$_2$O$_3$ is a well-known good oxygen diffusion barrier and may protect the Si surface from undesirable oxidation [10–12], it is expected that adding Al to HfO$_2$ to form hafnium aluminate films, as one possible solution, may reduce the oxygen diffusion coefficient. Recent experimental studies [13–18] have demonstrated that the hafnium aluminate films exhibit much stronger resistance to oxygen diffusion than HfO$_2$ and obstruct the growth of interfacial layers between hafnium aluminate and the Si substrate. However the mechanism of this effect of Al addition on the oxygen diffusion has not been well understood yet. In order to shed more light on the microscopic pictures of the oxygen diffusion in hafnium aluminate and effectively control the oxygen diffusion in oxides, we have performed density functional theory (DFT) calculations in conjunction with the climbing-image nudged elastic band (CI-NEB) method [19, 20] to study the diffusion of interstitial oxygen atoms and ions in monoclinic HfO$_2$ and the effects of Al addition.

2. Computational method

All calculations are performed using the plane wave pseudopotential method with the generalized gradient approximation (GGA) [21], as implemented in the Vienna *ab initio* simulation package (VASP) [22]. Electron–ion interaction is represented by the ultrasoft Vandelbilt pseudopotential [23, 24]. The

Table 1. Calculated formation energies (ΔE_f, in eV) of neutral interstitial oxygen and its defect complex formed with substitutional Al for Hf in monoclinic HfO_2 under oxygen-rich conditions. The binding sites of interstitial oxygen, the nearest distances (d_{O_i-Hf} and d_{O_i-O}, in Å) between interstitial oxygen and lattice atoms, and the bond lengths between interstitial oxygen and substitutional Al (d_{O_i-Al}, in Å) are also presented. O3 and O4 denote the threefold- and fourfold-coordinated lattice oxygen atoms in monoclinic HfO_2, respectively.

				ΔE_f	
Defect	Binding site	d_{O_i-O}	d_{O_i-Hf} (d_{O_i-Al})	Present	Ref. [28]
O_i	O3	1.50	2.16	1.67	1.6
O_i	O4	1.49	2.29	2.42	2.3
O_2	O3	1.54	2.17	2.14	2.1
O_i-Al_{Hf}	O3	1.42	2.50 (1.89)	2.98	
O_i-Al_{Hf}	O4	1.45	2.09 (2.66)	3.11	
O_2-Al_{Hf}	O3	1.41	2.79 (1.87)	5.56	

wavefunctions are expanded in plane waves up to a cutoff of 500 eV. For the calculations of oxygen diffusion, a monoclinic HfO_2 supercell containing 32 HfO_2 formula units (32 Hf and 64 O atoms) is used as the host structure, and one more oxygen atom is added. One of the Hf atoms is substituted by an Al atom in this supercell to model the Al addition. Due to the large size of the supercell, a single Γ point is employed for k-point sampling with an energy convergence of 9 meV/HfO_2. The diffusion pathway and the diffusion barrier of the interstitial oxygen atoms are determined by seeking the minimum energy path from one site to an adjacent site with the CI-NEB method [19, 20] as implemented in VASP [25]. The five images are initialized by linear interpolation between the two relaxed end points. Each of the images is relaxed until the atomic and spring forces are less than 0.02 eV Å^{-1}. A neutralizing background is applied to the supercell in the calculations for interstitial oxygen in a charged state. The Coulomb interaction between charged defects in different periodic cells is calculated using the Makov–Payne scheme [26], and the corresponding image charge correction is below 0.1 eV due to the large size of the supercell separating the periodic defect images by over 10 Å.

For the lattice parameters of the monoclinic phase of HfO_2 we obtain $a = 5.133$ Å, $b = 5.188$ Å, $c = 5.301$ Å, and $\beta = 99.79°$, in good agreement with the experimental values ($a = 5.199$ Å, $b = 5.170$ Å, $c = 5.298$ Å, and $\beta = 99.18°$) [27] and other GGA calculation results [28, 29]. The indirect band gap from Γ to B of monoclinic HfO_2 is 3.80 eV, which is lower than the experimental value of 5.68 eV, but is consistent with other *ab initio* GGA calculations [29].

3. Results and discussion

Lattice oxygen atoms in the monoclinic phase of HfO_2 are characterized by threefold-and fourfold-coordinated sites, both of which could potentially act as defect sites [28]. In addition, the incorporation of oxygen into HfO_2 may be from an atomic or molecular source. We have calculated the defect formation energies for interstitial oxygen point defects for atomic oxygen and molecular oxygen under oxygen-rich conditions, as listed in table 1. We find that an additional oxygen atom is energetically more favorable for binding the threefold-coordinated lattice oxygen atom, and the formation energy of the interstitial O_2 molecule is about 0.47 eV per atom

Table 2. Calculated exchange activation barriers (E_{ex}, in eV) of interstitial oxygen in different charge states in monoclinic HfO_2 without and with Al substitution (the latter case is labeled as HfO_2:Al). The calculated data from other work [30] are also shown, in parentheses, for comparison.

	Property	O_i^0	O_i^-	O_i^{2-}
E_{ex}	HfO_2	0.7 (0.8)	0.1 (0.3)	0.2 (0.6)
	HfO_2:Al	1.2	1.4	1.5

higher than that of the interstitial oxygen atom, consistently with a previous study of monoclinic HfO_2 [28]. These findings indicate that atomic oxygen would be the most important diffusion species in HfO_2, and the most important diffusion path for atomic oxygen would be through the interstitial sites around threefold-coordinated lattice oxygen atoms. If one of the lattice Hf atoms near the interstitial oxygen is substituted by an Al atom, the defect formation energy of the interstitial oxygen atom is still lower than that of an interstitial O_2 molecule under oxygen-rich conditions (see table 1). This suggests that the presence of Al in HfO_2 does not change the features of interstitial oxygen, including its form and site. Hence in this study we will focus on the more stable defect sites and the diffusion of interstitial oxygen atoms in HfO_2 with and without the Al substitution.

Previous DFT calculations [30] show that the favored mechanism of oxygen diffusion in HfO_2 is the diffusion of interstitial oxygen via exchange with lattice oxygen sites. This oxygen exchange mechanism is supported by more recent experimental studies [6, 9, 31, 32] on oxygen diffusion in HfO_2 films, with annealing in $^{18}O_2$. In order to understand the exchange mechanism of oxygen diffusion, we first follow the procedure in [30] for determining the diffusion barrier of interstitial oxygen in a range of charge states. The calculated barriers for interstitial oxygen atom and ions, via the exchange mechanism, are listed in table 2; these give the same trend as the previously calculated values [30]. We also find that the interstitial oxygen ion in the singly negatively charged state (O_i^-) has the smallest diffusion barrier. If one of the lattice Hf atoms near the interstitial oxygen during the diffusion is substituted by an Al atom, the diffusion barrier of oxygen increases by about 0.5 or 1.3 eV depending on the charge state of the interstitial oxygen (see table 2).

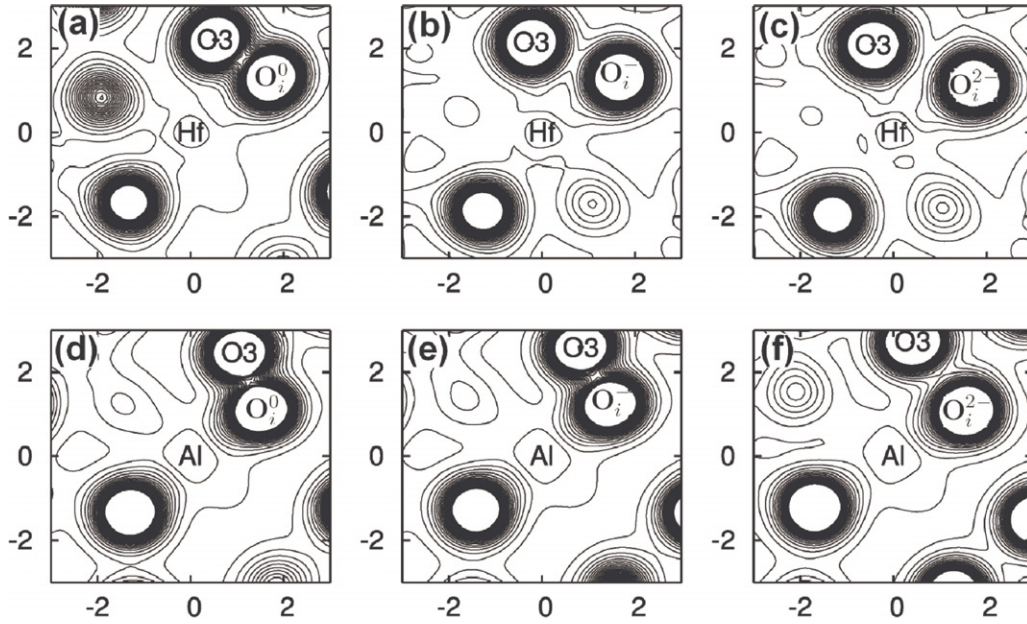In order to understand the effect of Al substitution on the diffusion barriers for interstitial oxygen, we examine

Figure 1. Charge density in the cross-section planes for interstitial oxygen point defects and their defect complexes with substitutional Al for Hf in HfO$_2$ in equilibrium: (a) O$_i^0$, (b) O$_i^-$, (c) O$_i^{2-}$, (d) (O$_i$–Al$_{Hf}$)^0, (e) (O$_i$–Al$_{Hf}$)$^-$, and (f) (O$_i$–Al$_{Hf}$)$^{2-}$. O3 and O$_i$ in the figures denote the threefold-coordinated lattice oxygen atom and interstitial oxygen atom, respectively.
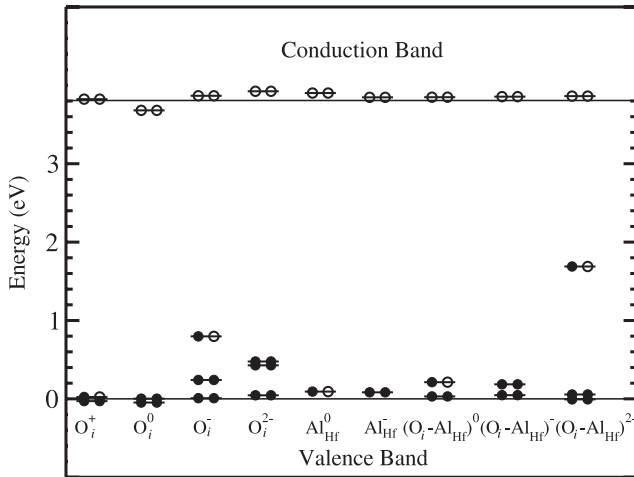

Figure 2. Schematic representation of the single-electron energy levels induced in the band gap of monoclinic HfO$_2$ by the interstitial oxygen (O$_i$), Al substituting for Hf (Al$_{Hf}$), and their defect complexes. Filled and open dots indicate occupied and unoccupied states, respectively. Note that the lowest unoccupied states near the bottom of the conduction band for O$_i^+$, O$_i^0$, (O$_i$–Al$_{Hf}$)^0, and (O$_i$–Al$_{Hf}$)$^-$ show the p orbital character of the oxygen atom, while others show the d orbital character of the Hf atom.

the electronic structures of the interstitial oxygen and substitutional Al for Hf as well as their defect complexes in equilibrium. Figure 1(a) shows the charge density in the plane, containing the lattice Hf atom, the threefold-coordinated oxygen atom (labeled as O3), and the interstitial oxygen atom in the neutral state. The interstitial oxygen atom forms a strong bond with the lattice oxygen atom, and the corresponding bond length is about 1.50 Å, almost equal to that of a free O$_2^{2-}$ ion.

When one electron is added to the interstitial oxygen atom to form an O$_i^-$ ion, the bond length between the lattice oxygen atom and O$_i^-$ increases to 2.07 Å, as shown in figure 1(b). When two electrons are added so as to form the O$_i^{2-}$ ion, the separation is increased further to 2.35 Å. The bond lengths between the interstitial oxygen and lattice Hf atom are 2.16 Å, 2.07 Å, and 2.08 Å for neutral, singly negatively, and doubly negatively charged states of O$_i$, respectively. This means that additional electrons transferred to interstitial oxygen atoms have little effect on the interaction between the interstitial oxygen atoms and lattice Hf atoms, but have an obvious effect on the bonding between lattice oxygen atoms and interstitial oxygen atoms. This effect can also be seen from the evolution of defect levels induced in the band gap by interstitial oxygen. Figure 2 illustrates schematically the single-electron energy level induced in the band gap of monoclinic HfO$_2$ and by the interstitial oxygen point defects. For neutral interstitial oxygen, due to the formation of oxygen dimer (O$_i$–O3), there appear two antibonding ppπ^* orbitals close to the valence band maximum (VBM) and unoccupied antibonding ppσ^* states near the bottom of the conduction band. For the singly negatively charged state of interstitial oxygen (O$_i^-$), the additional electron is added to the unoccupied antibonding ppσ^* states of the (O$_i$–O3) dimer; hence the bond between the lattice oxygen atom and interstitial oxygen is weak. The large separation between O$_i$ and O3 also leads to a downward shift of the half-occupied ppσ^* energy level to 0.8 eV above the VBM. For the doubly negatively charged state of interstitial oxygen (O$_i^{2-}$), the additional electron fills up the ppσ^* state, making the interstitial oxygen ion and lattice oxygen atom weakly bonded. Correspondingly, the highest occupied states of O$_i^{2-}$ drop to 0.48 eV above the VBM.

Substitution of an Al atom for one of the Hf atoms, i.e. Al$_{Hf}$, will create a shallow acceptor level close to the

VBM, and contribute a hole, as shown in figure 2. In particular, neutral Al_{Hf} and O_i, each bonded with lattice oxygen, attract each other, forming the defect complex $(Al_{Hf}^- - O_i^+)$. Figures 1(d), (e) and (f) clearly show the strong directional bonding of interstitial oxygen to substitutional Al atoms. The bond lengths between the substitutional Al atom and interstitial oxygen are 1.89 Å, 1.92 Å, and 1.91 Å for defect complexes $(O_i-Al_{Hf})^0$, $(O_i-Al_{Hf})^-$, and $(O_i-Al_{Hf})^{2-}$, respectively. This indicates that once one of the lattice Hf atoms around the interstitial oxygen is substituted by an Al atom, the interstitial oxygen atom will be strongly attracted by a neighboring substitutional Al atom. As noted above, Al substituting for Hf acts as an acceptor and contributes a hole, resulting in the $pp\pi^*$ state of the O_i-O3 dimer being half-occupied in the presence of Al_{Hf}. It behaves more like an oxygen dimer in singly positively charged $(O_i-O3)^+$, as shown in figure 2, and the bond length between the interstitial oxygen and the lattice oxygen atom is reduced to about 1.42 Å. Similarly, in the complex $(O3-O_i-Al_{Hf})^-$, the additional electron fills the $pp\pi^*$ level of the oxygen dimer, making the (O_i-O3) bond weaker. The bond length between the O_i atom and lattice oxygen atom increases to 1.48 Å, which is still shorter than that for the case without substitutional Al. If one more electron is added to the interstitial oxygen to form the complex $(O3-O_i-Al_{Hf})^{2-}$, it will be on the antibonding $pp\sigma^*$ state of the oxygen dimer, making the oxygen bond even weaker and shifting the $pp\sigma^*$ level to 1.70 eV above the VBM; this is accompanied by a larger separation of about 2.01 Å between the interstitial oxygen and lattice oxygen atom. Since the interstitial oxygen and lattice oxygen atom 'prefer' to form a shorter dimer in the case with substitutional Al, especially for the neutral and singly negatively charged states, the bonding between the interstitial oxygen and lattice oxygen atom becomes stronger for interstitial oxygen point defects in HfO_2 after Al addition. Therefore, substitution of Al for a lattice Hf atom increases the diffusion barrier of interstitial oxygen.

4. Conclusions

In summary, using *ab initio* total energy calculations we have studied the diffusion of interstitial oxygen atoms and ions in monoclinic HfO_2 with and without Al substitution. The present results show that Al substituting for Hf increases the diffusion barrier of interstitial oxygen. On the basis of the defect energy levels and the charge distribution for each interstitial oxygen defect and their complex defects with Al substituting for Hf, the bonding characters are analyzed. The increase of the diffusion barrier of interstitial oxygen can be explained by the interstitial oxygen being strongly attracted by its neighboring substitutional Al atoms, and the bonding between interstitial and lattice oxygen atoms being enhanced for each charge state of the interstitial oxygen point defects.

References

[1] Kingon A I, Maria J P and Streiffer S K 2000 *Nature* **406** 1032
[2] Wilk G D, Wallace R M and Anthony J M 2001 *J. Appl. Phys.* **89** 5243
[3] Robertson J 2000 *J. Vac. Sci. Technol.* B **18** 1785
[4] Copel M, Gribelyuk M and Gusev E 2000 *Appl. Phys. Lett.* **76** 436
[5] Intel 2006 Meet the world's first 45nm processor (January 2006) See, for example http://www.intel.com/technology/silicon/45nm_technology.htm
[6] Ferrari S and Scarel G 2004 *J. Appl. Phys.* **96** 144
[7] Green M L, Gusev E P, Degraeve R and Garfunkel E L 2001 *J. Appl. Phys.* **90** 2057
[8] Lee B H, Kang L, Nieh R, Qi W J and Lee J C 2000 *Appl. Phys. Lett.* **76** 1926
[9] Bastos K P, Morais J, Miotti L, Pezzi R P, Soares G V, Baumvol I J R, Hegde R I, Tseng H H and Tobin P J 2002 *Appl. Phys. Lett.* **81** 1669
[10] Gusev E P, Copel M, Cartier E, Baumvol I J R, Krug C and Gribelyuk M A 2000 *Appl. Phys. Lett.* **76** 176
[11] Copel M, Cartier E, Gusev E P, Guha S, Bojarczuk N and Poppeller M 2001 *Appl. Phys. Lett.* **78** 2670
[12] Hong Y E, Kim Y S, Do K, Lee D, Ko D H, Ku J H and Kim H 2005 *J. Vac. Sci. Technol.* A **23** 1413
[13] Zhu W J, Tamagawa T, Gibso M, Furukawa T and Ma T P 2002 *IEEE Electron Device Lett.* **23** 649
[14] Yu H Y, Li M F, Cho B J, Yeo C C, Joo M S, Kwong D L, Pan J S, Ang C H, Zheng J Z and Ramanathan S 2002 *Appl. Phys. Lett.* **81** 376
[15] Afanas'ev V V, Stesmans A and Tsai W 2003 *Appl. Phys. Lett.* **82** 245
[16] Yu H Y, Wu N, Li M F, Zhu C X, Cho B J, Kwong D L, Tung C H, Pan J S, Chai J W, Wang W D, Chi D Z, Ang C H, Zheng J Z and Ramanathan S 2002 *Appl. Phys. Lett.* **81** 3618
[17] Chang H S, Hwang H, Cho M, Kim H K and Moon D W 2004 *J. Vac. Sci. Technol.* A **22** 165
[18] Li Q *et al* unpublished In our experiments, we observed that adding Al to the HfO_2 film significantly suppresses the formation of interfacial oxide when the as-deposited film is annealed at 800 °C and at ambient condition
[19] Henkelman G and Jónsson H 2000 *J. Chem. Phys.* **113** 9978
[20] Henkelman G, Uberuaga B P and Jónsson H 2000 *J. Chem. Phys.* **113** 9901
[21] Perdew J P, Chevary J A, Vosko S H, Jackson K A, Pederson M R, Singh D J and Fiolhais C 1992 *Phys. Rev.* B **46** 6671
[22] Kresse G and Furthmüller J 1996 *Phys. Rev.* B **54** 11169
[23] Vanderbilt D 1990 *Phys. Rev.* B **41** 7892
[24] Kresse G and Hafner J 1994 *J. Phys.: Condens. Matter* **6** 8245
[25] *Manual of VASP and document of VASP Transition State Theory (TST) Tools* see the websites: http://cms.mpi.univie.ac.at/vasp/vasp/vasp.html http://theory.cm.utexas.edu/vtsttools/ respectively
[26] Makov G and Payne M C 1995 *Phys. Rev.* B **51** 4014
[27] Wang J, Li H P and Stevens R 1992 *J. Mater. Sci.* **27** 5397

[28] Foster A S, Lopez Gejo F, Shluger A L and
　　　 Nieminen R M 2002 *Phys. Rev.* B **65** 174117
[29] Kang J, Lee E C and Chang K J 2003 *Phys. Rev.* B
　　　 68 054106
[30] Foster A S, Shluger A L and Nieminen R M 2002 *Phys. Rev.
　　　 Lett.* **89** 225901

[31] Goncharova L V, Dalponte M, Starodub D G, Gustafsson T,
　　　 Garfunkel E, Lysaght P S, Foran B, Barnett J and
　　　 Bersuker G 2006 *Appl. Phys. Lett.* **89** 044108
[32] Zhao M, Nakajima K, Suzuki M, Kimura K, Uematsu M,
　　　 Torii K, Kamiyama S, Nara Y, Watanabe H, Shiraishi K,
　　　 Chikyow T and Yamada K 2007 *Appl. Phys. Lett.* **90** 133510